An Observer-Based Optimal Voltage Control Scheme for Three-Phase UPS Systems

Eun-Kyung Kim, Francis Mwasilu, Han Ho Choi, *Member, IEEE*, and Jin-Woo Jung, *Member, IEEE*

***Abstract*—This paper proposes a simple optimal voltage control method for three-phase uninterruptible-power-supply systems. The proposed voltage controller is composed of a feedback control term and a compensating control term. The former term is designed to make the system errors converge to zero, whereas the latter term is applied to compensate for the system uncertainties. Moreover, the optimal load current observer is used to optimize system cost and reliability. Particularly, the closed-loop stability of an observer-based optimal voltage control law is mathematically proven by showing that the whole states of the augmented observer-based control system errors exponentially converge to zero. Unlike previous algorithms, the proposed method can make a tradeoff between control input magnitude and tracking error by simply choosing proper performance indexes. The effectiveness of the proposed controller is validated through simulations on MATLAB/Simulink and experiments on a prototype 600-VA testbed with a TMS320LF28335 DSP. Finally, the comparative results for the proposed scheme and the conventional feedback linearization control scheme are presented to demonstrate that the proposed algorithm achieves an excellent performance such as fast transient response, small steady-state error, and low total harmonic distortion under load step change, unbalanced load, and nonlinear load with the parameter variations.**

***Index Terms*—Optimal load current observer, optimal voltage control, three-phase inverter, total harmonic distortion (THD), uninterruptible power supply (UPS).**

Nomenclature

V_i	Line-to-neutral inverter voltage vector ($\mathrm{V}_i = [v_{iA}\ v_{iB}\ v_{iC}]^T$).
$\mathrm{V}_{i\alpha\beta}$	Voltage vector in the $\alpha-\beta$ frame of $\mathrm{V}_i(V_{i\alpha\beta} = [v_{i\alpha}\ v_{i\beta}]^T$).
$\mathrm{V}^*_{i\alpha\beta}$	Reference voltage vector of $\mathrm{V}_{i\alpha\beta}(\mathrm{V}^*_{i\alpha\beta} = [v^*_{i\alpha}\ v^*_{i\beta}]^T)$.
V_{idq}	Voltage vector in the $d-q$ frame of $\mathrm{V}_i(\mathrm{V}_{idq} = [v_{id}\ v_{iq}]^T)$.
V^*_{idq}	Reference voltage vector of $\mathrm{V}_{idq}(\mathrm{V}^*_{idq} = [v^*_{id}\ v^*_{iq}]^T)$.
I_i	Inverter phase current vector ($\mathrm{I}_i = [i_{iA}\ i_{iB}\ i_{iC}]^T$).
I_{idq}	Current vector in the $d-q$ frame of $\mathrm{I}_i(\mathrm{I}_{idq} = [i_{id}\ i_{iq}]^T)$.
I^*_{idq}	Reference current vector of $\mathrm{I}_{idq}(\mathrm{I}^*_{idq} = [i^*_{id}\ i^*_{iq}]^T)$.
V_L	Line-to-neutral load voltage vector ($\mathrm{V}_L = [v_{LA}\ v_{LB}\ v_{LC}]^T$).
V_{Ldq}	Voltage vector in the $d-q$ frame of $\mathrm{V}_L(\mathrm{V}_{Ldq} = [v_{Ld}\ v_{Lq}]^T)$.
V^*_{Ldq}	Reference voltage vector of $\mathrm{V}_{Ldq}(\mathrm{V}^*_{Ldq} = [v^*_{Ld}\ v^*_{Lq}]^T)$.
I_L	Load current vector ($\mathrm{I}_L = [i_{LA}\ i_{LB}\ i_{LC}]^T$).
I_{Ldq}	Current vector in the $d-q$ frame of $\mathrm{I}_L(\mathrm{I}_{Ldq} = [i_{Ld}\ i_{Lq}]^T)$.
$\hat{\mathrm{I}}_{Ldq}$	Estimated current vector of $\mathrm{I}_{Ldq}(\hat{\mathrm{I}}_{Ldq} = [\hat{i}_{\mathrm{Ld}}\ \hat{i}_{\mathrm{Ld}}]^T)$.
ω	Angular frequency ($\omega = 2\pi f$).
f	Fundamental frequency ($f = 60$ Hz).
V_{dc}	DC-link voltage.
L_f	Filter inductance.
C_f	Filter capacitance.

Manuscript received April 3, 2014; revised June 23, 2014; accepted July 22, 2014. Date of publication August 26, 2014; date of current version March 6, 2015. This work was supported by the National Research Foundation of Korea under Grant 2012R1A2A2A01045312 funded by the Korea government (Ministry of Science, ICT and Future Planning).

The authors are with the Division of Electronics and Electrical Engineering, Dongguk University, Seoul 100-715, Korea (e-mail: jinwjung@dongguk.edu).

Color versions of one or more of the figures in this paper are available online at http://ieeexplore.ieee.org.

Digital Object Identifier 10.1109/TIE.2014.2351777

I. Introduction

UNINTERRUPTIBLE power supply (UPS) systems supply emergency power in case of utility power failures. Recently, the importance of the UPS systems has been intensified more and more due to the increase of sensitive and critical applications such as communication systems, medical equipment, semiconductor manufacturing systems, and data processing systems [1]–[3]. These applications require clean power and high reliability regardless of the electric power failures and distorted utility supply voltage. Thus, the performance of the UPS systems is usually evaluated in terms of the total harmonic distortion (THD) of the output voltage and the transient/steady-state responses regardless of the load conditions: load step change, linear load, and nonlinear load [4]–[7]. To improve the aforementioned performance indexes, a number of control algorithms have been proposed such as proportional–integral (PI) control, H_∞ loop-shaping control, model predictive control, deadbeat control, sliding-mode control, repetitive control, adaptive control, and feedback linearization control (FLC).

The conventional PI control suggested in [8] and [9] is easy to implement; however, the THD value of the output voltage is not low under a nonlinear-load condition. In [10], the H_∞ loop-shaping control scheme is described and implemented on a single-phase inverter, which has a simple structure and is robust against model uncertainties. A model predictive control method for UPS applications is described in [11]. By using a load current observer in place of current sensors, the authors claimed a reduced system cost. However, the simulation and experimental results do not reveal an exceptional performance in terms of THD and steady-state error. In [12], the deadbeat control method uses the state feedback information to compensate for

the voltage drop across the inductor. However, this method exhibits sensitivity to parameter mismatches, and the harmonics of the inverter output voltage are not very well compensated. In [13] and [14], the sliding-mode control technique reflects robustness to the system noise, and still, the control system has a well-known chattering problem. In [15], repetitive control is applied to achieve a high-quality sinusoidal output voltage of a three-phase UPS system. Generally, this control technique has a slow response time. In [16], the adaptive control method with low THD is proposed; nevertheless, there is still a risk of divergence if the controller gains are not properly selected. Multivariable FLC is presented in [17]. In this control technique, the nonlinearity of the system is considered to achieve low THD under nonlinear load. However, it is not easy to carry out due to the computation complexities. As a result, the aforementioned linear controllers are simple, but the performance is not satisfactory under nonlinear load. In contrast, the nonlinear controllers have an outstanding performance, but the implementation is not easy due to the relatively complicated controllers.

So far, the optimal control theory has been researched in various fields such as aerospace, economics, physics, and so on [18], since it has a computable solution called a performance index that can quantitatively evaluate the system performance by contrast with other control theories. In addition, the optimal control design gives the optimality of the controller according to a quadratic performance criterion and enables the control system to have good properties such as enough gain and phase margin, robustness to uncertainties, good tolerance of nonlinearities, etc. [19]. Hence, a linear optimal controller has not only a simple structure in comparison with other controllers but also a remarkable control performance similar to other nonlinear controllers [20]–[22].

Therefore, this paper proposes an observer-based optimal voltage control scheme for three-phase UPS systems. This proposed voltage controller encapsulates two main parts: a feedback control term and a compensating control term. The former term is designed to make the system errors converge to zero, and the latter term is applied to estimate the system uncertainties. The Lyapunov theorem is used to analyze the stability of the system. Specially, this paper proves the closed-loop stability of an observer-based optimal voltage control law by showing that the system errors exponentially converge to zero. Moreover, the proposed control law can be systematically designed taking into consideration a tradeoff between control input magnitude and tracking error unlike previous algorithms [23]. The efficacy of the proposed control method is verified via simulations on MATLAB/Simulink and experiments on a prototype 600-VA UPS inverter testbed with a TMS320LF28335 DSP. In this paper, a conventional FLC method in [17] is selected to demonstrate the comparative results because it has a good performance under a nonlinear-load condition, and its circuit model of a three-phase inverter in [17] is similar to our system model. Finally, the results clearly show that the proposed scheme has a good voltage regulation capability such as fast transient behavior, small steady-state error, and low THD under various load conditions such as load step change, unbalanced load, and nonlinear load in the existence of the parameter variations.

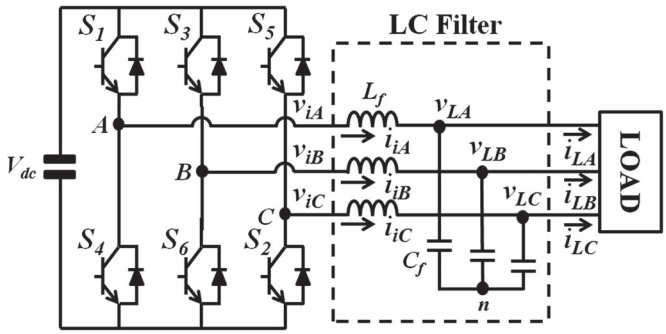

Fig. 1. Three-phase inverter with an LC filter for a UPS system.

II. System Description and Problem Formulation

The three-phase UPS system with an LC filter is shown in Fig. 1, which is composed of a dc-link voltage $(V_{\rm dc})$, a three-phase pulsewidth modulation (PWM) inverter $(S_1 \sim S_6)$, an output LC filter (L_f, C_f), and a three-phase load (e.g., linear or nonlinear load).

Based on Fig. 1, the dynamic model of a three-phase inverter can be derived in a $d-q$ synchronous reference frame as follows [24]:

$$\begin{cases} \dot{i}_{id} = \omega i_{iq} + k_2 v_{id} - k_2 v_{Ld} \\ \dot{i}_{iq} = -\omega i_{id} + k_2 v_{iq} - k_2 v_{Lq} \end{cases}, \quad \begin{cases} \dot{v}_{Ld} = \omega v_{Lq} + k_1 i_{id} - k_1 i_{Ld} \\ \dot{v}_{Lq} = -\omega v_{Ld} + k_1 i_{iq} - k_1 i_{Lq} \end{cases} \tag{1}$$

where $k_1 = 1/C_f$, and $k_2 = 1/L_f$. In system model (1), v_{Ld}, v_{Lq}, i_{id}, and i_{iq} are the state variables, and v_{id} and v_{iq} are the control inputs. In this scheme, the assumption is made to construct the optimal voltage controller and optimal load current observer as follows:

1) The load currents (i_{Ld} and i_{Lq}) are unknown and vary very slowly during the sampling period [11].

III. Proposed Optimal Voltage Controller Design and Stability Analysis

A. Optimal Voltage Controller Design

Here, a simple optimal voltage controller is proposed for system (1). First, let us define the $d-q$-axis inverter current references (i_{id}^*, i_{iq}^*) as

$$i_{id}^* = i_{Ld} - \frac{1}{k_1}\omega v_{Lq}^*, \quad i_{iq}^* = i_{Lq} + \frac{1}{k_1}\omega v_{Ld}^*. \tag{2}$$

Then, the error values of the load voltages and inverter currents are set as

$$\begin{aligned} v_{de} &= v_{Ld} - v_{Ld}^*, \quad v_{qe} = v_{Lq} - v_{Lq}^* \\ i_{de} &= i_{id} - i_{id}^*, \quad i_{qe} = i_{iq} - i_{id}^*. \end{aligned} \tag{3}$$

Therefore, system model (1) can be transformed into the following error dynamics:

$$\dot{x} = Ax + B(u + u_d) \tag{4}$$

where $x = [v_{de}\ v_{qe}\ i_{de}\ i_{qe}]^T$, $u = [v_{id}\ v_{iq}]^T$, $u_d = [d_d\ d_q]^T$,

$$A = \begin{bmatrix} 0 & \omega & k_1 & 0 \\ -\omega & 0 & 0 & k_1 \\ -k_2 & 0 & 0 & 0 \\ 0 & -k_2 & 0 & 0 \end{bmatrix}, \quad B = \begin{bmatrix} 0 & 0 \\ 0 & 0 \\ k_2 & 0 \\ 0 & k_2 \end{bmatrix}$$

$d_q = -v_{Ld}^* + (1/k_2)\omega i_{Lq}$, and $d_q = -v_{Lq}^* + (1/k_2)\omega i_{Ld}$. Note that u_d is applied to compensate for the system uncertainties as a compensating term.

Consider the following Riccati equation for the solution matrix P [25]:

$$PA + A^T P - PBR^{-1}B^T P + Q = 0 \tag{5}$$

where Q and R are the positive definite weighting matrices with sufficient dimensions.

Remark 1: Recall that Q and R are the weighting matrices [26]. Excessive large error or control input values can be penalized by using properly chosen Q and R. Generally, the large Q means a high control performance, whereas the large R means a small input magnitude. Consequently, there is a tradeoff between Q and R in the control system. The Q and R parameters generally need to be tuned until satisfactory control results are obtained.

Let the diagonal matrices Q and R be defined as

$$Q = \begin{bmatrix} Q_1 & 0 & 0 & \dots & 0 \\ 0 & Q_2 & 0 & \dots & 0 \\ \dots & \dots & \dots & \dots & \dots \\ 0 & \dots & \dots & 0 & Q_m \end{bmatrix}$$

$$R = \begin{bmatrix} R_1 & 0 & 0 & \dots & 0 \\ 0 & R_2 & 0 & \dots & 0 \\ \dots & \dots & \dots & \dots & \dots \\ 0 & \dots & \dots & 0 & R_k \end{bmatrix}$$

where Q and R have positive diagonal entries such that $\sqrt{Q_i} = 1/y_i^{\max}$, where $i = 1, 2, \dots, m$, and $\sqrt{R_i} = 1/u_i^{\max}$, where $i = 1, 2, \dots, m$. The number $y_i^{\max}$ is the maximally acceptable deviation value for the ith component of output y. The other quantity $u_i^{\max}$ is the ith component of input u. With an initial guessed value, the diagonal entries of Q and R can be adjusted through a trial-and-error method.

Then, the optimal voltage controller can be designed by the following equation:

$$u = -u_d + Kx \tag{6}$$

where $K = -R^{-1}B^T P$ denotes the gain matrix, and u_d and Kx represent a feedforward control term and a feedback control term, respectively.

Remark 2: The proposed voltage controller, in essence, is designed based on the well-known linear quadratic regulator minimizing the following performance index [27]:

$$J = \int_0^\infty \left(x^T Q x + u_n^T R u_n\right) dt \tag{7}$$

where x is the error, $u_n = u + u_d$, and Q and R are symmetrical positive definite matrices as mentioned above.

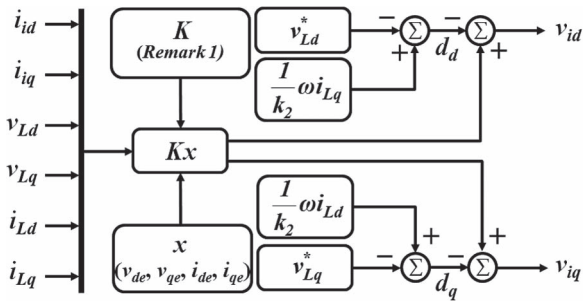

Fig. 2. Block diagram of the proposed optimal voltage control scheme.

B. Stability Analysis of Voltage Controller

Consider the following Lyapunov function:

$$V(x) = x^T P x. \tag{8}$$

From (4)–(6), and (8), the time derivative of $V(x)$ is given by the following:

$$\begin{aligned} \dot{V}(x) &= \frac{d}{dt}x^T P x = 2x^T P(A + BK)x \\ &= 2x^T P(A - BR^{-1}B^T P)x \\ &= x^T(PA + A^T P - 2PBR^{-1}B^T P)x \le -x^T Q x. \end{aligned} \tag{9}$$

This implies that x exponentially converges to zero.

Remark 3: By considering the parameter variations, the state-dependent coefficient matrix A is rewritten as $A' = A + \Delta A$, where ΔA means the value of system parameter variations. Thus, (4) can be transformed into the following error dynamics:

$$\dot{x} = A'x + B(u + u_d). \tag{10}$$

The new time derivative of (8) is given by the following:

$$\begin{aligned} \dot{V}(x) &= 2x^T P\dot{x} \\ &= x^T(PA + P\Delta A + \Delta A^T P + A^T P \\ &\quad - 2PBR^{-1}B^T P)x < 0. \end{aligned} \tag{11}$$

By (5), (11) is reduced to

$$\dot{V}(x) = x^T(P\Delta A + \Delta A^T P - Q - PBR^T B^T P)x. \tag{12}$$

If the following inequality holds for the given ΔA:

$$P\Delta A + \Delta A^T P < PBR^{-1}B^T P + Q \tag{13}$$

then $\dot{V} < 0$ for all nonzero x. Therefore, the proposed optimal voltage control system can tolerate any parameter variation satisfying (13).

Fig. 2 shows the block diagram of the proposed optimal voltage control scheme.

IV. Optimal Load Current Observer Design and Stability Analysis

A. Optimal Load Current Observer Design

As seen in (2) and (4), the inverter current references (i_d^* and i_q^*) and feedforward control term (u_d) need load current information as inputs. To avoid using current sensors, a linear optimal load current observer is introduced in this algorithm.

From (1) and the assumption, the following dynamic model is obtained to estimate the load current:

$$\begin{cases} \dot{x}_o = A_o x_o + B_o u_o \\ y = C_o x_o \end{cases} \tag{14}$$

where $x_o = [i_{Ld}\ i_{Lq}\ v_{Ld}\ v_{Lq}]^T$, $u_o = [k_1 i_{id}\ k_1 i_{iq}]^T$,

$$A_o = \begin{bmatrix} 0 & 0 & 0 & 0 \\ 0 & 0 & 0 & 0 \\ -k_1 & 0 & 0 & \omega \\ 0 & -k_1 & -\omega & 0 \end{bmatrix},\ B_o = C_o^T = \begin{bmatrix} 0 & 0 \\ 0 & 0 \\ 1 & 0 \\ 0 & 1 \end{bmatrix}.$$

Then, the load current observer is expressed as

$$\dot{\hat{x}}_o = A_o \hat{x}_o + B_o u_o - L(y - C_o \hat{x}_o) \tag{15}$$

where $\hat{x}_0 = [\hat{i}_{Ld}\ \hat{i}_{Lq}\ \hat{v}_{Ld}\ \hat{v}_{Lq}]^T$, and $\hat{i}_{Ld}$ and $\hat{x}_{Lq}$ are estimates of i_{Ld} and i_{Lq}, respectively. In addition, L is an observer gain matrix calculated by

$$L = -P_o C_o^T R_o^{-1} \tag{16}$$

and P_o is the solution of the following Riccati equation:

$$A_o P_o + P_o A_o^T - P_o C_o^T R_o^{-1} C_o P_o + Q_o = 0 \tag{17}$$

where Q_o and R_o are the positive definite weighting matrices with sufficient dimensions. The manner of choosing Q_o and R_o is the same as in Remark 1.

Remark 4: The fourth-order Kalman–Bucy optimal observer [19] is used to minimize the performance index $E(x_e^T x_e)$, where $x_e = x_o - \hat{x}_o$, representing the expectation value of $x_e^T x_e$ for the following perturbed model:

$$\dot{x}_o = A_o x_o + B_o u_o + d, \quad y = C_o x_o + v \tag{18}$$

where $d \in R^4$ and $v \in R^2$ are independent white Gaussian noise signals with $E(d) = 0$, $E(v) = 0$, $E(dd^T) = Q_o$, and $E(vv^T) = R_o$.

B. Stability Analysis of Load Current Observer

The error dynamics of the load current observer can be obtained as follows:

$$\dot{x}_e = (A - LC)x_e. \tag{19}$$

Define the Lyapunov function as

$$V_o(x_e) = x_e^T X x_e \tag{20}$$

where $X = P_o^{-1}$. Its time derivative along the error dynamics (19) is represented by the following:

$$\begin{aligned} \dot{V}_o(\tilde{x}) &= \frac{d}{dt} x_e^T X x_e = 2x_e^T \left(X A_o - X P_o C_o^T R_o^{-1} C_o\right) x_e \\ &= x_e^T X \left(A_o P_o + P_o A_o^T - 2 P_o C_o^T R_o^{-1} C_o P_o\right) X x_e \\ &\le -x_e^T X Q_o X x_e. \end{aligned} \tag{21}$$

This implies that x_e exponentially converges to zero. ■

V. Observer-Based Control Law and Closed-Loop Stability Analysis

A. Observer-Based Control Law

With the estimated load currents achieved from the observer instead of the measured quantities, the inverter current errors and feedforward control term can be obtained as follows:

$$\begin{aligned} \bar{i}_{de} &= i_{id} - \hat{i}_{Ld} + \frac{1}{k_1}\omega v_{Lq}^*, \quad \bar{i}_{qe} = i_{iq} - \hat{i}_{Lq} - \frac{1}{k_1}\omega v_{Ld}^* \\ \bar{d}_d &= -v_{Ld}^* + \frac{1}{k_2}\omega \hat{i}_{Lq}, \quad \bar{d}_q = -v_{Lq}^* - \frac{1}{k_2}\omega \hat{i}_{Ld}. \end{aligned} \tag{22}$$

Then, (22) can be rewritten as the following equations:

$$\begin{aligned} \bar{i}_{de} &= i_{de} + [1 \quad 0 \quad 0 \quad 0] x_e \\ \bar{i}_{qe} &= i_{qe} + [0 \quad 1 \quad 0 \quad 0] x_e \\ \bar{d}_d &= d_d + \frac{\omega}{k_2}[0 \quad 1 \quad 0 \quad 0] x_e \\ \bar{d}_q &= d_q - \frac{\omega}{k_2}[1 \quad 0 \quad 0 \quad 0] x_e. \end{aligned} \tag{23}$$

From (6) and (23), the proposed observer-based control law can be achieved as

$$u = -\bar{u}_d + K\bar{x} \tag{24}$$

where $\bar{x} = [v_{de}\ v_{qe}\ \bar{i}_{de}\ \bar{i}_{qe}]^T$, and $\bar{u}_d = [\bar{d}_d\ \bar{d}_q]^T$.

B. Closed-Loop Stability Analysis

For the purpose of analyzing the stability, (24) is rewritten as the following:

$$u = -u_d + Kx + Hx_e \tag{25}$$

where $H = (\omega/k_2)E + KF$, $\bar{x} = x + Fx_e$,

$$E = \begin{bmatrix} 0 & 1 & 0 & 0 \\ -1 & 0 & 0 & 0 \end{bmatrix},\ \text{and } F = \begin{bmatrix} 0 & 0 & 0 & 0 \\ 0 & 0 & 0 & 0 \\ 1 & 0 & 0 & 0 \\ 0 & 1 & 0 & 0 \end{bmatrix}.$$

Let us define the Lyapunov equation as

$$V(x, x_e) = x^T P x + \zeta x_e^T P_0^{-1} x_e \tag{26}$$

where ζ is a scalar quantity that satisfies the following inequality:

$$\zeta > \frac{\|PBH\|^2}{[\lambda_{\min}(Q) \cdot \lambda_{\min}(P_o^{-1} Q_o P_o^{-1})]}. \tag{27}$$

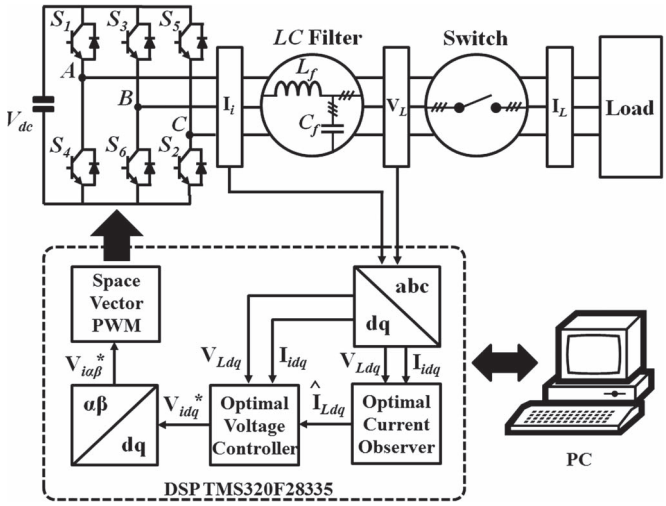

Fig. 3. Block diagram of the proposed observer-based optimal voltage control system.

TABLE I
SYSTEM PARAMETERS OF A 600-VA TESTBED

Parameters	Descriptions	Values	Units
V_{dc}	dc-link voltage	290	[V]
T_s	Sampling time	200	[μs]
f_s	Switching frequency	5	[kH]
f_1	Fundamental frequency	60	[Hz]
$V_{L,\,rms}$	Load output voltage	110	[V]
L_f	Output filter inductance	10	[mH]
C_f	Output filter capacitance	7	[μF]
R_L	Resistance for linear load	60	[Ω]
R_{load}	Resistance for nonlinear load	200	[Ω]
C_{load}	Capacitance for nonlinear load	650	[μF]
L_{load}	Inductance for nonlinear load	4	[mH]

Then, the time derivative of the Lyapunov equation is given by

$$\begin{aligned}\dot{V} &= 2x^T P(Ax+Bu+Bu_d)+2\zeta x_e^T P_o^{-1}(A_o+LC_o)x_e \\ &= 2x^T P(Ax+BKx+BHx_e)+2\zeta x_e^T P_o^{-1}(A_o+LC_o)x_e \\ &\le -x^T Qx+2x^T PBHx_e-\zeta x_e^T P_o^{-1}Q_oP_o^{-1}x_e \\ &\le -\lambda_{\min}(Q)\|x\|^2+2\|PBH\|\cdot\|x\|\cdot\|x_e\| \\ &\quad -\zeta\lambda_{\min}\left(P_o^{-1}Q_oP_o^{-1}\right)\|x_e\|^2\le 0. \end{aligned} \tag{28}$$

This implies that x and x_e exponentially go to zero.

As a result, the design procedure of the proposed observer-based control law can be summarized as follows.

Step 1) Build system model (1) in the $d-q$ coordinate frame and then derive error dynamics (4) by using system parameters.

Step 2) Set the optimal voltage controller (6) with the feedforward control term (u_d) and feedback control term (Kx).

Step 3) Define the load current estimation model (14) and build the load current observer (15) by using the Kalman–Bucy optimal observer.

Step 4) Select the observer weighting matrices Q_o and R_o in Riccati equation by referring to Remark 1. Then, choose the observer gain L in (16) using Q_o and R_o.

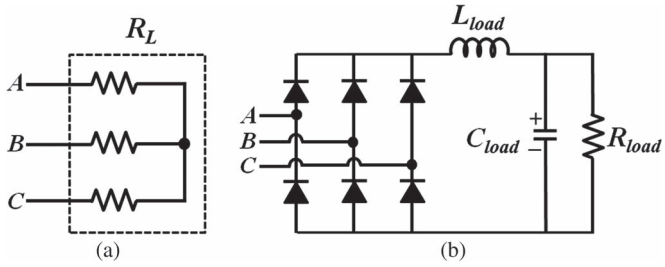

Fig. 4. Two types of load circuits. (a) Resistive linear load. (b) Nonlinear load with a three-phase diode rectifier.

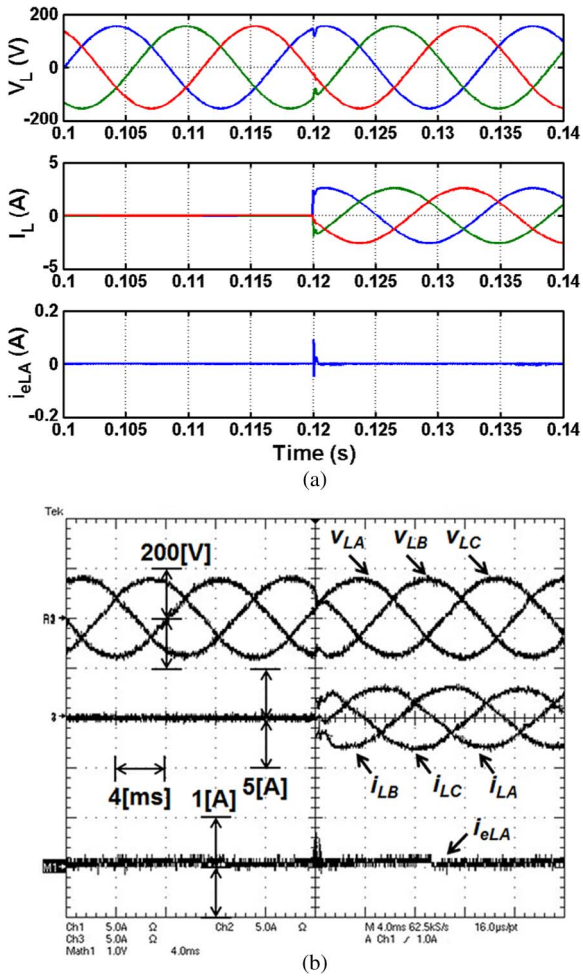

Fig. 5. Simulation and experimental results of the proposed observer-based optimal voltage control scheme under load step change with -30% parameter variations in L_f and C_f (i.e., balanced resistive load: 0%–100%)—First: Load output voltages (V_L), Second: Load output currents (I_L), Third: Phase A load current error $(i_{eLA}=i_{LA}-\hat{i}_{LA})$. (a) Simulation. (b) Experiment.

Step 5) Select the controller weighting matrices Q and R in Riccati equation by referring to Remark 1. Then, choose the control gain K in (6) using Q and R.

VI. PERFORMANCE VALIDATIONS

A. Testbed Description

The proposed observer-based optimal voltage controller has been performed through both simulations with MATLAB/Simulink and experiments with a prototype 600-VA UPS inverter testbed. Moreover, the conventional FLC scheme [17] is adopted to exhibit a comparative analysis of the proposed

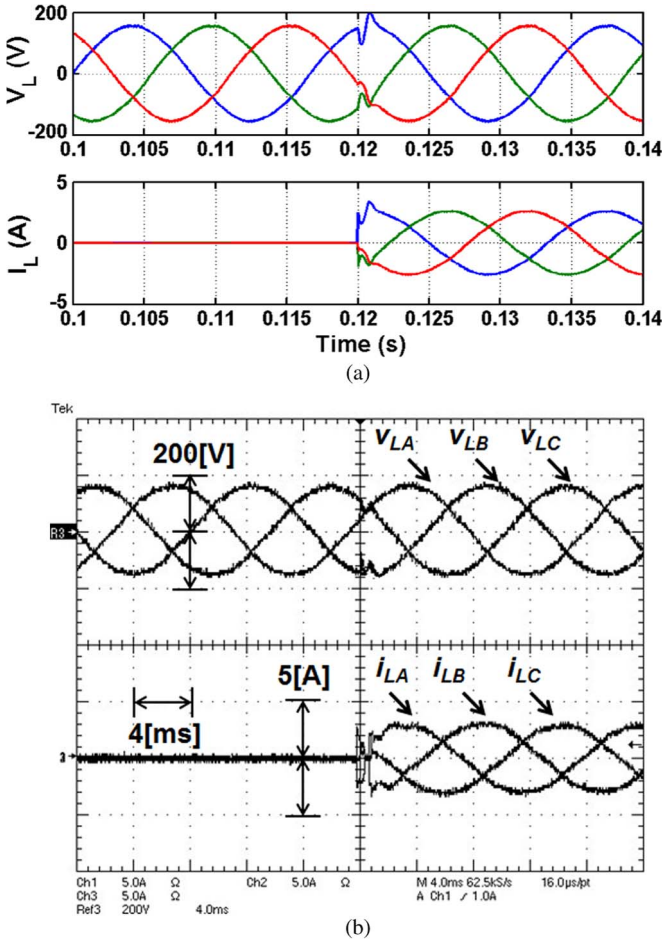

Fig. 6. Simulation and experimental results of the conventional FLC scheme under load step change with -30% parameter variations in L_f and C_f (i.e., balanced resistive load: 0%–100%)—First: Load output voltages (V_L), Second: Load output currents (I_L). (a) Simulation. (b) Experiment.

control scheme since it reveals a reasonable performance for nonlinear load and has the circuit model of a three-phase inverter similar to our system. Fig. 3 illustrates the overall block diagram to carry out the proposed algorithm using a 16-bit floating-point TMS320LF28335 DSP. In the testbed, the inverter phase currents and line-to-neutral load voltages are measured via the CTs and PTs to implement the feedback control. In this paper, a space vector PWM technique is used to generate the control inputs ($V_{i\alpha}$ and $V_{i\beta}$) in real time. Table I lists all system parameters used in this study.

The proposed algorithm is verified through two different types of loads as explicitly depicted in Fig. 4. More specifically, Fig. 4(a) shows a linear-load circuit that consists of a resistor per phase, whereas Fig. 4(b) depicts a nonlinear-load circuit that is comprised of a three-phase full-bridge diode rectifier, an inductor (L_{load}), a capacitor (C_{load}), and a resistor (R_{load}). Note that during simulation and the experiment, observer gain L and controller gain K are selected based on Remark 1 as

$$L = 10^5 \begin{bmatrix} -1.0029 & 0.0003 \\ -0.0003 & -1.0029 \\ 1.1877 & 0 \\ 0 & 1.1877 \end{bmatrix}$$

$$K = 10^{11} \begin{bmatrix} 0.3241 & 0 & 3.1623 & 0 \\ 0 & 0.3241 & 0 & 3.1623 \end{bmatrix}.$$

TABLE II
STEADY-STATE PERFORMANCES OF THE PROPOSED AND CONVENTIONAL SCHEMES

Control Scheme			The Proposed Observer-Based Optimal Voltage Control Scheme		
Load Condition			Step change	Unbalanced	Nonlinear
THD (%)	Simulation		0.11	0.13	0.89
	Experiment		0.89	0.91	1.72
Load RMS Voltages (V)	Simulation	v_{LA}	109.9	109.9	109.6
		v_{LB}	109.8	110.0	109.5
		v_{LC}	110.0	109.9	109.8
	Experiment	v_{LA}	109.9	109.9	109.4
		v_{LB}	109.9	109.8	109.5
		v_{LC}	109.7	109.8	109.7
Control Scheme			The Conventional FLC Scheme		
Load Condition			Step change	Unbalanced	Nonlinear
THD (%)	Simulation		0.94	0.97	1.96
	Experiment		1.32	1.39	2.98
Load RMS Voltages (V)	Simulation	v_{LA}	109.7	109.8	109.3
		v_{LB}	110.0	109.9	109.3
		v_{LC}	109.8	109.9	109.3
	Experiment	v_{LA}	109.8	109.9	109.3
		v_{LB}	109.8	109.8	109.2
		v_{LC}	109.7	109.7	109.3

B. Simulation and Experimental Results

The proposed voltage control algorithm is carried out in various conditions (i.e., load step change, unbalanced load, and nonlinear load) to impeccably expose its merits. In order to instantly engage and disengage the load during a transient condition, the on–off switch is employed as shown in Fig. 3. The resistive load depicted in Fig. 4(a) is applied under both the load step change condition (i.e., 0%–100%) and the unbalanced load condition (i.e., phase B opened) to test the robustness of the proposed scheme when the load is suddenly disconnected. In practical applications, the most common tolerance variations of the filter inductance (L_f) and filter capacitance (C_f), which are used as an output filter, are within $\pm 10\%$. To further justify the robustness under parameter variations, a 30% reduction in both L_f and C_f is assumed under all load conditions such as load step change, unbalanced load, and nonlinear load.

Fig. 5 shows the simulation and experimental results of the proposed control method during the load step change. Moreover, Fig. 6 presents the comparative results obtained by employing the conventional FLC scheme under the same condition. Specifically, the figures display the load voltages (First waveform: $\mathbf{V_L}$), load currents (Second waveform: $\mathbf{I_L}$), and phase A load current error (Third waveform: $i_{eLA} = i_{LA} - \hat{i}_{LA}$). It is important to note that the load current error waveform in the results of the conventional FLC method is not included because the FLC scheme does not need load current information. It can be observed in Fig. 5 that when the load is suddenly changed, the load output voltage presents little distortion. However, it quickly returns to a steady-state condition in 1.0 ms, as

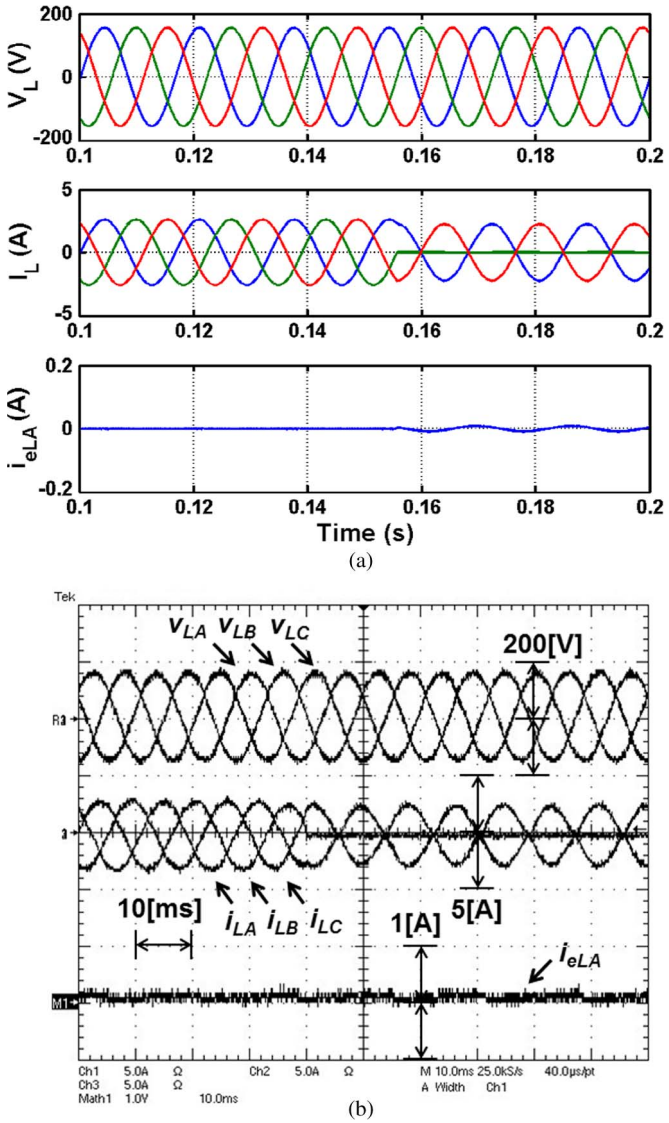

Fig. 7. Simulation and experimental results of the proposed observer-based optimal voltage control scheme under unbalanced load with -30% parameter variations in L_f and C_f (i.e., phase B opened)—First: Load output voltages (V_L), Second: Load output currents (I_L), Third: Phase A load current error $(i_{eLA} = i_{LA} - \hat{i}_{LA})$. (a) Simulation. (b) Experiment.

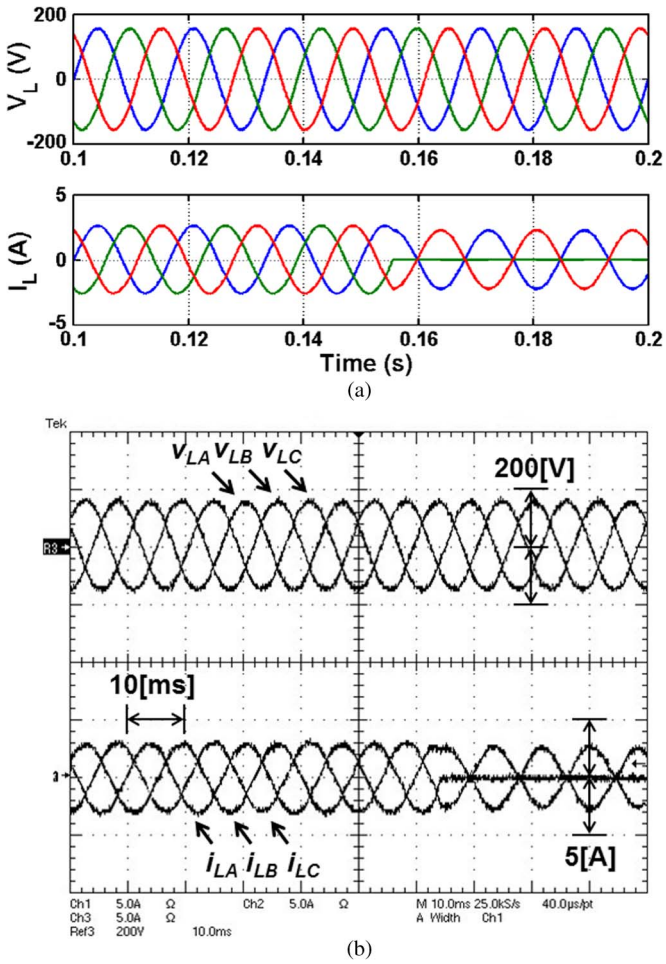

Fig. 8. Simulation and experimental results of the conventional FLC scheme under unbalanced load with -30% parameter variations in L_f and C_f (i.e., phase B opened)—First: Load output voltages (V_L), Second: Load output currents (I_L). (a) Simulation. (b) Experiment.

shown in the simulation results in Fig. 5(a). Moreover, it has revealed a fast recovery time of 1.5 ms in a real experimental setup as shown in Fig. 5(b). Conversely, as illustrated in the simulation results in Fig. 6(a), voltage distortion is larger, and its recovery time of 1.4 ms is much longer as compared with that in Fig. 5(a). Moreover, Fig. 6(b) shows a longer recovery time of 2.0 ms than that observed in Fig. 5(b). On the other hand, the THD values of the load output voltage at steady-state full-load operation are presented in Table II. These values are found as 0.11% for simulation and 0.89% for experiment using the proposed scheme. However, the conventional FLC scheme shows 0.94% and 1.32% for the case of simulation and experiment, respectively. Therefore, it is explicitly demonstrated that the proposed algorithm attains lower THD. It can be observed from Table II that the load root mean square (RMS) voltage values in both schemes are appropriately regulated at steady state. Moreover, the third waveform in Fig. 5 shows a small load current error (i_{eLA}) between the measured value (i_{LA}) and the estimated value $(\hat{i}_{LA})$.

Next, the characteristic performances of the transient and steady state under unbalanced load are verified through Figs. 7 and 8. Precisely, this case is implemented under a full-load condition by suddenly opening phase B. It is shown that the load output voltages are controlled well, although the rapid change in the load current of phase B is observed as it is opened. As shown in Fig. 7, the respective THD values of the output voltage are 0.13% for the simulation and 0.91% for the experiment obtained by using the proposed method. However, the THD values are 0.97% and 1.39%, respectively, for the simulation and experiment in case of the conventional FLC scheme, as depicted in Fig. 8. As given in Table II, small steady-state voltage errors under unbalanced load are observed because the load RMS voltage values of both methods are almost 110 V. In addition, the load current observer provides high-quality information to the proposed controller as portrayed in Fig. 7.

To evaluate the steady-state performance under nonlinear load, a three-phase diode rectifier shown in Fig. 4(b) is used. The simulation and experimental results of each control method under this condition are demonstrated in Figs. 9 and 10. To this end, the THD values of the load voltage waveforms achieved

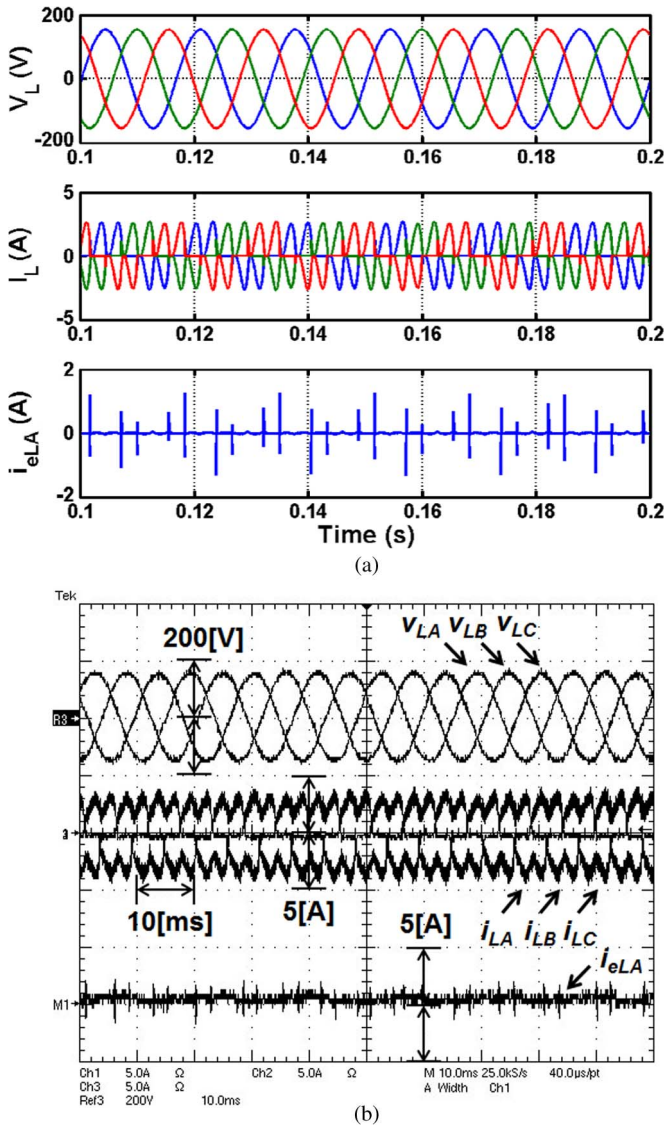

Fig. 9. Simulation and experimental results of the proposed observer-based optimal voltage control scheme under nonlinear load with -30% parameter variations in L_f and C_f (i.e., three-phase diode rectifier)—First: Load output voltages (V_L), Second: Load output currents (I_L), Third: Phase A load current error $(i_{eLA} = i_{LA} - \hat{i}_{LA})$. (a) Simulation. (b) Experiment.

with the proposed scheme are 0.89% for simulation and 1.72% for experiment, respectively. In the case of the conventional FLC scheme, the corresponding load voltage THD values are 1.96% for simulation and 2.98% for experiment, respectively. It can be also observed that the proposed control strategy provides a better load voltage regulation in steady state compared with the conventional FLC method. In Fig. 9, it can be evidently seen that the load current observer guarantees a good estimation performance because of a small load current error (i_{eLA}). Finally, all THD and load RMS voltage values under the three load conditions previously described are summarized in Table II.

VII. Conclusion

This paper has proposed a simple observer-based optimal voltage control method of the three-phase UPS systems The proposed controller is composed of a feedback control term to stabilize the error dynamics of the system and a compensating control term to estimate the system uncertainties. Moreover, the optimal load current observer was used to optimize system cost and reliability. This paper proved the closed-loop stability of an observer-based optimal voltage controller by using the Lyapunov theory. Furthermore, the proposed voltage control law can be methodically designed taking into account a tradeoff between control input magnitude and tracking error unlike previous algorithms. The superior performance of the proposed control system was demonstrated through simulations and experiments. Under three load conditions (load step change, unbalanced load, and nonlinear load), the proposed control scheme revealed a better voltage tracking performance such as lower THD, smaller steady-state error, and faster transient response than the conventional FLC scheme even if there exist parameter variations.

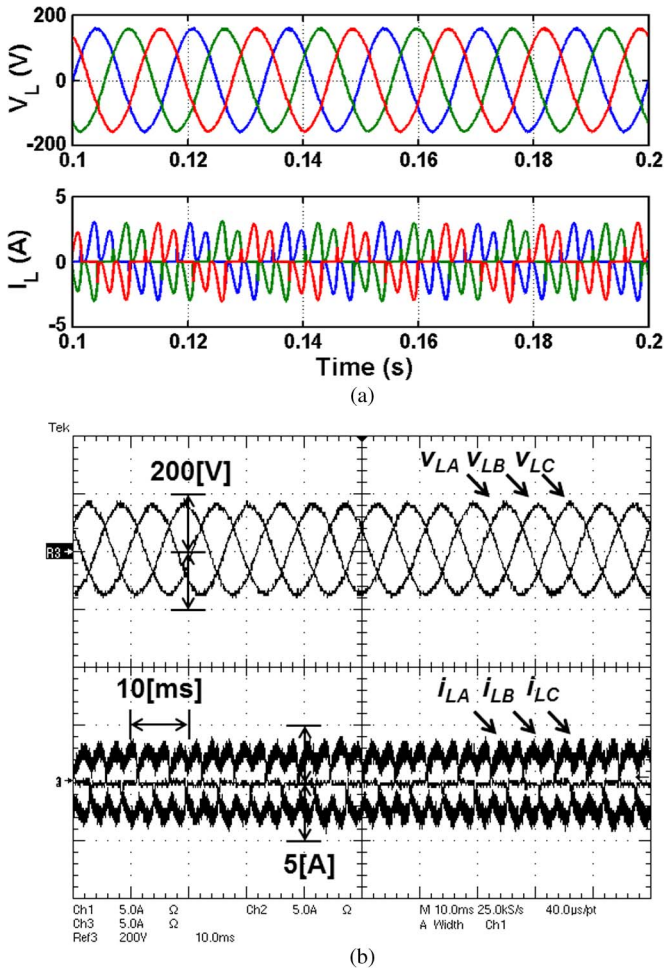

Fig. 10. Simulation and experimental results of the conventional FLC scheme under nonlinear load with -30% parameter variations in L_f and C_f (i.e., three-phase diode rectifier)—First: Load output voltages (V_L), Second: Load output currents (I_L). (a) Simulation. (b) Experiment.

References

[1] A. Nasiri, "Digital control of three-phase series-parallel uninterruptible power supply systems," *IEEE Trans. Power Electron.*, vol. 22, no. 4, pp. 1116–1127, Jul. 2007.

[2] Y. H. Chen and P. T. Cheng, "An inrush current mitigation technique for the line-interactive uninterruptible power supply systems," *IEEE Trans. Ind. Appl.*, vol. 46, no. 4, pp. 1498–1508, May/Jun. 2010.

[3] K. S. Low and R. Cao, "Model predictive control of parallel-connected inverters for uninterruptible power supplies," *IEEE Trans. Ind. Electron.*, vol. 55, no. 8, pp. 2884–2893, Aug. 2008.
[4] A. Mokhtarpour, H. A. Shayanfar, M. Bathaee, and M. R. Banaei, "Control of a single phase unified power quality conditioner-distributed generation based input output feedback linearization," *J. Elect. Eng. Technol.*, vol. 8, no. 6, pp. 1352–1364, Nov. 2013.
[5] J. H. Lee, H. G. Jeong, and K. B. Lee, "Performance improvement of grid-connected inverter systems under unbalanced and distorted grid voltage by using a PR controller," *J. Elect. Eng. Technol.*, vol. 7, no. 6, pp. 918–925, Nov. 2012.
[6] H. K. Kang, C. H. Yoo, I. Y. Chung, D. J. Won, and S. I. Moon, "Intelligent coordination method of multiple distributed resources for harmonic current compensation in a microgrid," *J. Elect. Eng. Technol.*, vol. 7, no. 6, pp. 834–844, Nov. 2012.
[7] C. Salim, B. M. Toufik, and G. Amar, "Harmonic current compensation based on three-phase three-level shunt active filter using fuzzy logic current controller," *J. Elect. Eng. Technol.*, vol. 6, no. 5, pp. 595–604, Sep. 2011.
[8] U. Borup, P. N. Enjeti, and F. Blaabjerg, "A new space-vector-based control method for UPS systems powering nonlinear and unbalanced loads," *IEEE Trans. Ind. Appl.*, vol. 37, no. 6, pp. 1864–1870, Nov./Dec. 2001.
[9] H. Karimi, A. Yazdani, and R. Iravani, "Robust control of an autonomous four-wire electronically-coupled distributed generation unit," *IEEE Trans. Power Del.*, vol. 26, no. 1, pp. 455–466, Jan. 2011.
[10] T. S. Lee, S. J. Chiang, and J. M. Chang, " H_∞ loop-shaping controller designs for the single-phase UPS inverters," *IEEE Trans. Power Electron.*, vol. 16, no. 4, pp. 473–481, Jul. 2001.
[11] P. Cortés *et al.*, "Model predictive control of an inverter with output LC filter for UPS applications," *IEEE Trans. Ind. Electron.*, vol. 56, no. 6, pp. 1875–1883, Jun. 2009.
[12] T. Kawabata, T. Miyashita, and Y. Yamamoto, "Dead beat control of three phase PWM inverter," *IEEE Trans. Power Electron.*, vol. 5, no. 1, pp. 21–28, Jan. 1990.
[13] H. Komurcugil, "Rotating sliding line based sliding mode control for single-phase UPS inverters," *IEEE Trans. Ind. Electron.*, vol. 59, no. 10, pp. 3719–3726, Oct. 2012.
[14] O. Kukrer, H. Komurcugil, and A. Doganalp, "A three-level hysteresis function approach to the sliding mode control of single-phase UPS inverters," *IEEE Trans. Ind. Electron.*, vol. 56, no. 9, pp. 3477–3486, Sep. 2009.
[15] G. Escobar, A. A. Valdez, J. Leyva-Ramos, and P. Mattavelli, "Repetitive-based controller for a UPS inverter to compensate unbalance and harmonic distortion," *IEEE Trans. Ind. Electron.*, vol. 54, no. 1, pp. 504–510, Feb. 2007.
[16] T. D. Do, V. Q. Leu, Y. S. Choi, H. H. Choi, and J. W. Jung., "An adaptive voltage control strategy of three-phase inverter for stand-alone distributed generation systems," *IEEE Trans. Ind. Electron.*, vol. 60, no. 12, pp. 5660–5672, Dec. 2013.
[17] D. E. Kim and D. C. Lee, "Feedback linearization control of three-phase," *IEEE Trans. Ind. Electron.*, vol. 57, no. 3, pp. 963–968, Mar. 2010.
[18] T. D. Do, S. Kwak, H. H. Choi, and J. W. Jung, "Suboptimal control scheme design for interior permanent-magnet synchronous motors: An SDRE-based approach," *IEEE Trans. Power Electron.*, vol. 29, no. 6, pp. 3020–3031, Jul. 2013.
[19] F. Lin, *Robust Control Design: An Optimal Control Approach*. Chichester, U.K.: Wiley, 2007.
[20] C. Olalla, R. Leyva, A. E. Aroudi, and I. Queinnec, "Robust LQR control for PWM converters: An LMI approach," *IEEE Trans. Ind. Electron.*, vol. 56, no. 7, pp. 2548–2558, Jul. 2009.
[21] P. Rao, M. L. Crow, and Z. Yang, "STATCOM control for power system voltage control applications," *IEEE Trans. Power Del.*, vol. 15, no. 4, pp. 1311–1317, Oct. 2000.
[22] Y. S. Rao and M. C. Chandokar, "Real-time electrical load emulator using optimal feedback control technique," *IEEE Trans. Ind. Electron.*, vol. 57, no. 4, pp. 1217–1225, Apr. 2010.
[23] T. Cimen, "State-dependent Riccati equation control: A survey," in *Proc. IFAC World Congr.*, Seoul, Korea, Jul. 2008, vol. 17, pp. 3761–3775.
[24] H. Tao, J. L. Duarte, and M. A. M. Hendrix, "Line-interactive UPS using a fuel cell as the primary source," *IEEE Trans. Ind. Electron.*, vol. 55, no. 8, pp. 3012–3021, Aug. 2008.
[25] B. D. O. Anderson and J. B. Moore, *Optimal Control: Linear Quadratic Methods*. Sydney, Australia: Prentice-Hall, 1990.
[26] O. H. Bosgra, H. Kwakernaak, and G. Meinsma, *Design Methods for Control Systems*. Delft, The Netherlands: DISC, 2001/2002.
[27] D. Xue, Y. Chen, and D. P. Atherton, *Linear Feedback Control: Analysis and Design with MATLAB*. Philadelpia, PA, USA: SIAM, 2007.

Eun-Kyung Kim received the B.S. degree in electrical engineering from Dongguk University, Seoul, Korea, in 2009, where she is currently working toward the Ph.D. degree in the Division of Electronics and Electrical Engineering.

From 2009 to 2012, she was with the Electrical Vehicle Research Laboratory, VCTech Company, Ltd., Gyeonggi, Korea. Her research interests include digital-signal-processor-based electric machine drives and control of distributed generation systems using renewable energy sources.

Francis Mwasilu received the B.S. degree in electrical engineering from the University of Dar es Salaam, Dar es Salaam, Tanzania, in 2008. He is currently working toward the Ph.D. degree in the Division of Electronics and Electrical Engineering, Dongguk University, Seoul, Korea.

From 2009 to 2011, he was a Utilities Engineer with JTI—Tanzania. His current research interests include distributed generation systems, electric vehicles, and renewable energy sources integration in modern power systems.

Han Ho Choi (M'03) received the B.S. degree in control and instrumentation engineering from Seoul National University, Seoul, Korea, in 1988 and the M.S. and Ph.D. degrees in electrical engineering from the Korea Advanced Institute of Science and Technology, Daejeon, Korea, in 1990 and 1994, respectively.

He is currently with the Division of Electronics and Electrical Engineering, Dongguk University, Seoul. His current research interests include control theory and its application to real-world problems.

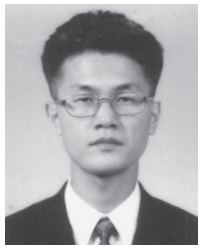

Jin-Woo Jung (S'97–M'06) received the B.S. and M.S. degrees in electrical engineering from Hanyang University, Seoul, Korea, in 1991 and 1997, respectively, and the Ph.D. degree in electrical and computer engineering from The Ohio State University, Columbus, OH, USA, in 2005.

From 1997 to 2000, he was with the Digital Appliance Research Laboratory, LG Electronics Co., Ltd., Seoul. From 2005 to 2008, he was a Senior Engineer with the R&D Center and with the PDP Development Team, Samsung SDI Co., Ltd., Korea. Since 2008, he has been an Associate Professor with the Division of Electronics and Electrical Engineering, Dongguk University, Seoul. His current research interests include digital-signal-processor-based electric machine drives, distributed generation systems using renewable energy sources, and power conversion systems and drives for electric vehicles.